Water-Based Thixotropic Polymer Gel Electrolyte for Dye-Sensitized Solar Cells

Se Jeong Park,[†,‡,∥] Kichoen Yoo,[†,§,∥] Jae-Yup Kim,[†] Jin Young Kim,[†,⊥] Doh-Kwon Lee,[†] BongSoo Kim,[†,⊥] Honggon Kim,[†,⊥] Jong Hak Kim,[§] Jinhan Cho,[‡] and Min Jae Ko[†,⊥,*]

[†]Photo-Electronic Hybrids Research Center, Korea Institute of Science and Technology (KIST), Seoul 136-791, Korea, [‡]Department of Chemical and Biological Engineering, Korea University, Anam-dong, Seongbuk-gu, Seoul 136-713, Korea, [§]Department of Chemical and Biomolecular Engineering, Yonsei University, Seoul 120-746, Korea, and [⊥]Green School, Korea University, 145, Anam-ro, Seongbuk-gu, Seoul 136-701, Korea. [∥]S. J. Park and K. Yoo contributed equally to this work.

ABSTRACT For the practical application of dye-sensitized solar cells (DSSCs), it is important to replace the conventional organic solvents based electrolyte with environmentally friendly and stable ones, due to the toxicity and leakage problems. Here we report a noble water-based thixotropic polymer gel electrolyte containing xanthan gum, which satisfies both the environmentally friendliness and stability against leakage and water intrusion. For application in DSSCs, it was possible to infiltrate the prepared electrolyte into the mesoporous TiO_2 electrode at the fluidic state, resulting in sufficient penetration. As a result, this electrolyte exhibited similar conversion efficiency (4.78% at 100 mW cm^{-2}) and an enhanced long-term stability compared to a water-based liquid electrolyte. The effects of water on the photovoltaic properties were examined elaborately from the cyclic voltammetry curves and impedance spectra. Despite the positive shift in the conduction band potential of the TiO_2 electrode, the open-circuit voltage was enhanced by addition of water in the electrolyte due to the greater positive shift in the I^-/I_3^- redox potential. However, due to the dye desorption and decreased diffusion coefficient caused by the water content, the short-circuit photocurrent density was reduced. These results will provide great insight into the development of efficient and stable water-based electrolytes.

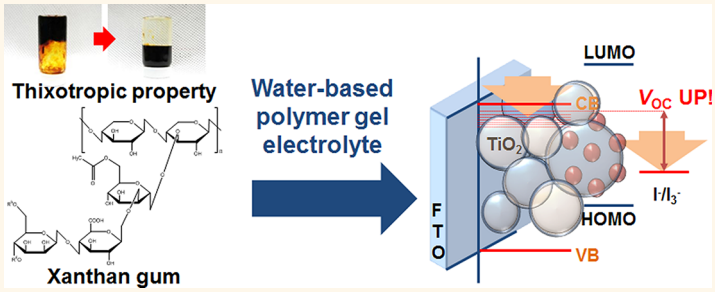

KEYWORDS: dye-sensitized solar cell · xanthan gum · thixotropic · polymer gel electrolyte · water-based electrolyte

Dye-sensitized solar cells (DSSCs) are prospective photovoltaic devices that provide high conversion efficiency, around 12%, with low cost and eco-friendly properties.[1,2] They are also transparent and can be produced in various colors, making it possible for them to be applied in building-integrated photovoltaic (BIPV) materials. In a conventional DSSC, an I^-/I_3^- redox electrolyte is located between the working and counter electrodes and plays an important role in regenerating oxidized dye molecules and in determining the photovoltage of the DSSC. Organic-solvent-based liquid electrolytes (*e.g.*, acetonitrile or 3-methoxypropionitrile) have conventionally been used in DSSCs; however, several organic solvents are toxic and/or explosive, which are obstacles to their practical application because of environmental and safety issues. Therefore, water-based solvents have recently been investigated to replace organic ones.[3−5] Water-based electrolytes are environmentally friendly, and the DSSCs employing water-based electrolytes are resistant to performance degradation caused by water intrusion through imperfect sealing.

However, liquid electrolytes have a fundamental limitation for long-term operation regardless of the kind of solvent due to their evaporation and leakage. Therefore, polymer gel electrolytes have recently received considerable attention because of their superior mechanical properties and long-term stability.[6−8] If the advantages of water-based electrolytes and polymer gel electrolytes could be combined, it would be possible to develop an environmentally friendly, highly reliable electrolyte that resists both water and solvent leakage.[9−12]

Under these circumstances, we have developed a noble water-based polymer gel electrolyte utilizing xanthan gum, which has a thixotropic property. Xanthan gum is a water-soluble, environmentally friendly polymer whose abundant hydroxyl groups form a

* Address correspondence to mjko@kist.re.kr.

Received for review January 9, 2013 and accepted April 17, 2013.

Published online April 25, 2013
10.1021/nn4001269

three-dimensional network. In addition, xanthan gum is thixotropic, which means that its viscosity decreases when an external stress is applied and recovers after a certain amount of time.[8] That is, it becomes liquid when shaken, stirred, or otherwise agitated and becomes a gel again upon resting for a certain amount of time. Polymer gel electrolytes generally do not penetrate very well into mesoporous TiO_2 electrodes in DSSCs because the radius of gyration of polymer chain in the electrolyte is larger than the pore size of the mesoporous TiO_2 electrodes.[6−8,13,14] However, because a xanthan-gum-based electrolyte has the thixotropic property, it could infiltrate as a liquid into a TiO_2 electrode, resulting in sufficient penetration into the TiO_2 electrode.[8,13−15] We prepared a water-based electrolyte comprising 50 wt % water with an organic solvent, *i.e.*, 3-methoxypropionitrile (MPN). In addition, a water-based polymer gel electrolyte was prepared by incorporating xanthan gum. The effects of water content in the electrolyte were examined focusing on the shift in the redox potential of I^-/I_3^- and the shift in the conduction band potential of the TiO_2 electrode. Furthermore, the photovoltaic properties including long-term stability were compared among the DSSCs employing a water-based liquid electrolyte (50 wt % of water content) and a water-based polymer gel electrolyte (50 wt % of water content with xanthan gum). A hydrophobic dye, TG6, was used as a sensitizer to prevent the dye desorption from the TiO_2 electrode.[16,17]

RESULTS AND DISCUSSION

Properties of Xanthan Gum. Figure 1a shows the chemical structure of xanthan gum, and Figure 1b shows the states of the water-based polymer gel electrolyte containing xanthan gum, before and after the electrolyte was shaken by hand.[18] The water-based polymer gel electrolyte was prepared by mixing a 3 wt % xanthan gum aqueous solution and an MPN-based solution containing the I^-/I_3^- redox couple and additives. The weight ratio of the xanthan gum to MPN solution was 1:1. The electrolyte was initially a gel. As shown in Figure 1b, the electrolyte containing xanthan gum lost its viscosity when it was shaken by hand. As the structure of the gel electrolyte was progressively broken down, the gel transformed into a fluidic sol. The electrolyte infiltrated as a fluidic sol into the DSSC so that the electrolyte could infiltrate easily and sufficiently penetrate into the mesoporous TiO_2 electrode. After a certain time, the xanthan gum in the electrolyte cross-linked, and the electrolyte became viscous again in the internal space between the working and counter electrodes, resulting in a gel state.[8,13] The thixotropic behavior of the electrolyte was quantitatively examined using a viscometer (Figure S1, Supporting Information). The electrolyte containing xanthan gum lost its viscosity progressively by the applied shear rate. The electrolyte then maintained its fluidity for a while, regardless of the change in the applied shear rate. The electrolyte then became viscous again after a certain amount of time.

Photovoltaic Properties. Before the photovoltaic performances of the electrolyte containing xanthan gum were characterized, the basic effects of the water content in the electrolyte on the DSSC were examined. Water-based liquid electrolytes were prepared by mixing the MPN-based electrolyte with various amounts of water. As shown in Figure S2 (Supporting Information), the water content in the electrolyte samples increased the open-circuit voltage (V_{oc}) of the DSSC by almost the same magnitude for all the samples except the sample containing 100 wt % MPN-based electrolyte. However, the short-circuit photocurrent density (J_{sc}) of the DSSC gradually deceased with increasing water concentration in the electrolyte. The decreased J_{sc} was attributed to the dye molecules to some extent being desorbed from the TiO_2 electrode (Figure S3, Supporting Information). As a result, the conversion efficiency (Eff) was highest for the DSSC employing the electrolyte containing 10 wt % water and was similar for DSSCs employing electrolytes containing up to 40 wt % water. However, Eff was greatly decreased for the DSSCs employing electrolytes containing more than 50 wt % water because J_{sc} was greatly reduced for those DSSCs. We chose the condition of 50 wt % water in order to prepare the water-based polymer gel electrolyte containing xanthan gum since the performance of electrolytes is too poor when they contain more than 50 wt % water, and the xanthan gum cannot be homogeneously dissolved in electrolytes containing less than 50 wt % water. Especially, the solubility of I_2 in MPN/water cosolvent is greatly reduced, and I_2 is even precipitated as water content increases over 50 wt %. We prepared the water-based polymer gel electrolyte (denoted as XG50) by mixing the 3 wt % xanthan gum aqueous solution with the water-based liquid electrolyte containing 50 wt % water (denoted as W50).

Figure 2 compares the $J-V$ curves for the DSSCs employing the W00 (anhydrous MPN-based electrolyte), W50, and XG50 electrolytes, and each parameter is listed in Table 1. As already confirmed, compared to the W00, the V_{oc} was higher and J_{sc} was significantly lower for the DSSCs employing either the W50 or XG50 electrolytes because of the water content. However, the fill factor (FF) was highly enhanced by the water content, resulting in 4.6% and 8.6% decreases in Eff for the W50 and XG50 electrolytes, respectively, compared to that for the W00 electrolyte. It is noteworthy that the XG50 exhibited a performance comparable with that of W50 in spite of the higher viscosity. The Eff of the DSSC with XG50 was only 4.2% less than that of the DSSC with W50, indicating that XG50 is a promising water-based polymer gel electrolyte. Judging from the almost same J_{sc} for both W50 and XG50 electrolytes, the XG50 electrolyte easily penetrated into the mesoporous TiO_2 electrode at room temperature, and the interfacial contact between the

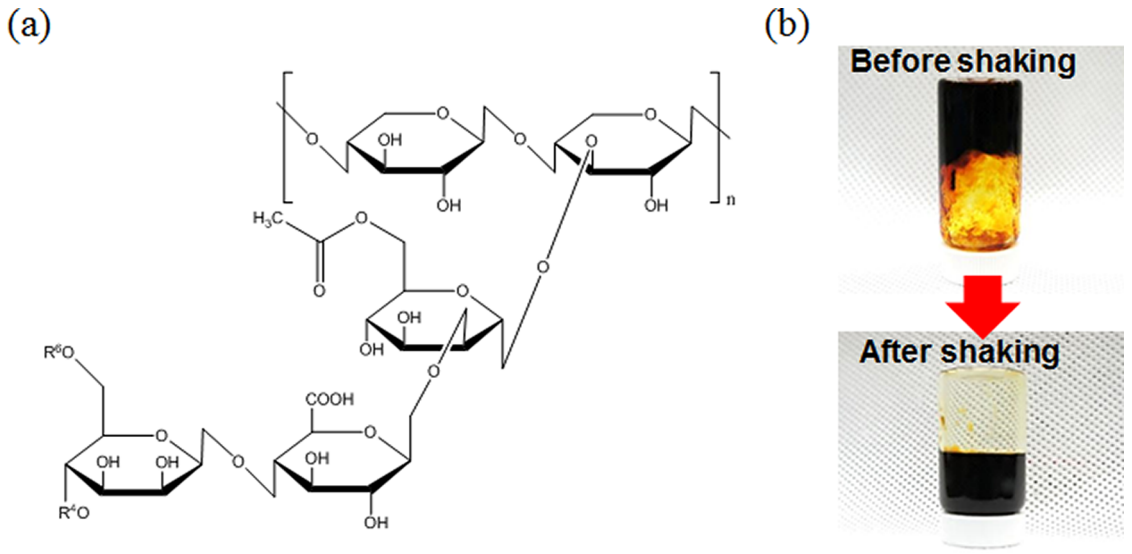

Figure 1. (a) Chemical structure of xanthan gum. (b) Photographs of water-based polymer gel electrolyte containing xanthan gum, taken before and after hand shaking.

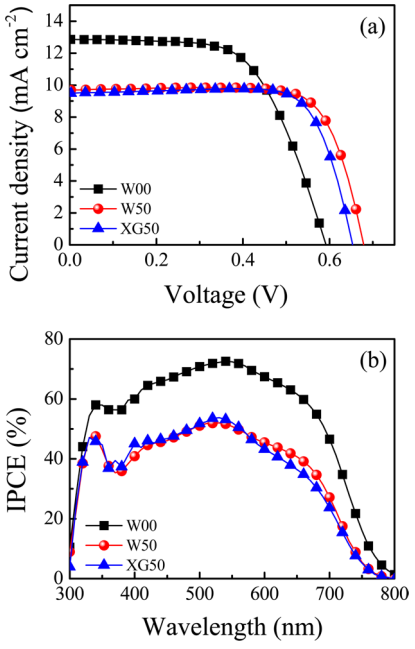

Figure 2. (a) $J-V$ curves for DSSCs employing different kinds of electrolytes under illumination (AM1.5, 100 mW cm^{-2}). Black squares represent reference electrolyte (W00); that is, MPN-based electrolyte without water content. Red circles represent water-based liquid electrolyte containing 50 wt % water (W50). Blue triangles represent water-based polymer gel electrolyte containing 50 wt % water and xanthan gum (XG50). (b) IPCE spectra for each cell.

TABLE 1. Summary of $J-V$ Characteristics for DSSCs Employing Different Kinds of Electrolytes (W00, W50, and XG50)

sample	J_{sc} (mA/cm^2)	V_{oc} (V)	FF	Eff (%)
W00	12.86	0.59	0.61	5.23
W50	9.69	0.68	0.76	4.99
XG50	9.49	0.65	0.77	4.78

TABLE 2. Diffusion Coefficients of Electrolytes (W00, W50, and XG50) Obtained from Impedance Spectra for Symmetric Dummy Cells with Pt-Coated FTO Glass Substrates

sample	diffusion coefficient[a] (cm^2/s)
W00	1.15×10^{-5}
W50	5.60×10^{-6}
XG50	3.78×10^{-6}

[a] Diffusion coefficients were calculated from the relation $D_n = L^2/(W_s - T)$. D_n and L represent the diffusion coefficient and distance between each electrode, respectively. $W_s - T$ is the parameter related to the finite Warburg impedance (W_s), which is determined by fitting impedance spectra.

electrolyte and TiO_2 electrode was sufficient, which was possible owing to the thixotropic property of xanthan gum.

J_{sc} Decrease. The enhanced V_{oc} and FF and the decreased J_{sc} were noticeable effects of the electrolytes that contained water. The decreased J_{sc} was related to the desorption of dye from the TiO_2 electrode, as already mentioned. Water generally attacks the linkage between a dye molecule and the TiO_2 electrode by hydrolysis.[9−12,19,20] To decrease the possibility of dye molecules being desorbed from the TiO_2 electrode, we used TG6, a hydrophobic dye; however, it was not possible to completely prevent the dye molecules from being desorbed from the TiO_2 electrode. In addition, the diffusion coefficient was decreased by the water of the electrolyte, which may affect J_{sc}. The diffusion coefficients obtained from the impedance spectra for symmetric dummy cells employing Pt-coated fluorine-doped tin oxide (FTO) glasses are listed in Table 2. The diffusion coefficients were significantly lower for the electrolytes that contained water.

V_{oc} Increase. V_{oc} was enhanced possibly as a result of (1) a positive shift in the redox potential for the I_3^-/I^- redox couple, (2) a negative shift in the conduction

band of the TiO_2 electrode, or (3) an increase in the recombination resistance between the electrolyte and the TiO_2 electrode.[4,5,20] First, we determined the redox potential (E_{redox}) of the electrolyte with and without water content using cyclic voltammetry (CV). It was carried out in MPN solutions containing the I^-/I_3^- redox couple with and without water content, at a scan rate of 50 mV s^{-1}. As shown in Figure 3, each CV curve typically exhibits two pairs of redox peaks for the I^-/I_3^- redox couple. E_{redox} for I^-/I_3^- was calculated from the redox peaks at the more negative potential.[21,22] As a result, E_{redox} for I^-/I_3^- was positively shifted by about 200 mV more for the electrolyte containing 50 wt % water (W50) than for the electrolyte without water (W00). The positive shift in E_{redox} is consistent with data in other reports and is considered to be the main reason for the enhanced V_{oc}.[4] The positive shift of E_{redox} by the water can affect the dye regeneration. It is known that the highest occupied molecular orbital (HOMO) energy level of TG6 is +1.02 V (*versus* NHE),[18] and the E_{redox} of I^-/I_3^- with organic solvent is about +0.35 V (*versus* NHE).[23] Because the E_{redox} of I^-/I_3^- was positively shifted by 200 mV in this study, the energy gap between the HOMO energy level of TG6 and E_{redox} of I^-/I_3^- was about 470 mV (1.02 V − 0.55 V). Recently, it was demonstrated that the dye can be efficiently regenerated with the energy gap of only 230 mV.[24] Therefore, it can be concluded that the energy gap of 470 mV is large enough for the efficient dye regeneration.

Electrochemical impedance spectra were then obtained to investigate the effects of water in the electrolyte on the conduction band edge of the TiO_2 electrode and the recombination resistance between the electrolyte and TiO_2 electrode. As shown in Figure S4 (Supporting Information), the chemical capacitance (C_μ) and charge recombination resistance (R_{ct}) were obtained for each electrolyte on the basis of bias voltage (V_{bias}). C_μ can be obtained from the constant phase element (CPE) in the equivalent circuit, which represents the interfacial capacitance. C_μ represents the charge density at the TiO_2 conduction band,[4,5,20] and V_{bias} represents the difference in potential between the quasi-Fermi level (E_{Fn}) of the TiO_2 electrode and E_{redox} of the electrolyte.[25] However, the effect of the decrease in voltage (V_{series}) caused by the total series resistance (R_{series}) should be eliminated to exactly evaluate the difference in potential applied between the TiO_2 electrode and the redox species. Therefore, the corrected bias voltage (V_F) can be calculated from the following equations:[26−29]

$$V_{bias} = V_F + V_{series} \quad (1)$$

$$V_{series} = [j/(j_{sc} - j)] \int_{j_{sc}}^{j} R_{series} dj \quad (2)$$

where j represents the photocurrent density at a given V_{bias} and j_{sc} represents the short-circuit current density.

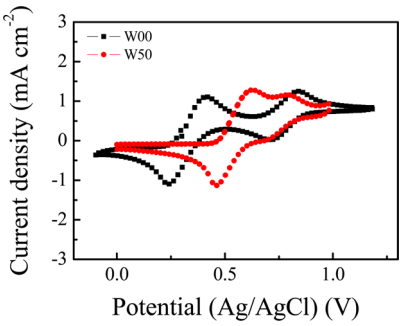

Figure 3. CV curves for the electrolytes of MPN solutions containing 0.1 M $LiClO_4$, 5 mM LiI, and 0.5 mM I_2 with (W50, water concentration was 50 wt %) and without (W00) water content, measured at a scan rate of 50 mV s^{-1}.

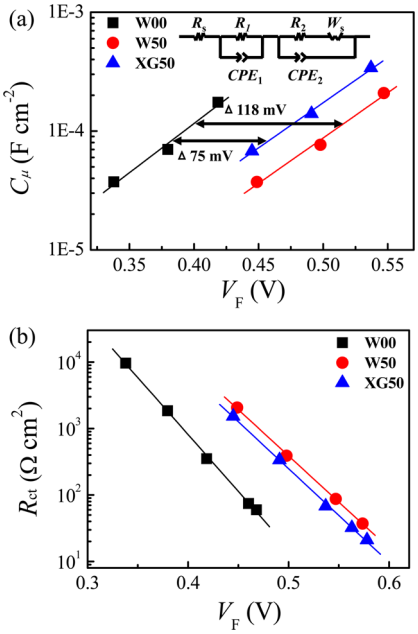

Figure 4. (a) Chemical capacitance (C_μ) (inset: equivalent circuit model) and (b) charge recombination resistance (R_{ct}) for the TiO_2 electrode employing different kinds of electrolyte, according to the corrected voltage (V_F). Each value was evaluated from the impedance spectra in the dark state.

R_{series} at a given V_{bias} can be calculated from the following equation:

$$R_{series} = R_{Pt} + R_s + R_d \quad (3)$$

R_{Pt} represents the interfacial resistance between the Pt counter electrode and the electrolyte. R_s and R_d represent the sheet resistance at the substrates and the resistance of electrolyte diffusion, respectively. These resistances can be obtained from the impedance spectra at the given V_{bias}.

The C_μ values obtained based on V_F are shown in Figure 4a. V_F can be regarded as nearly the exact difference in potential between E_{Fn} of the TiO_2 electrode and E_{redox} of the electrolyte, excluding voltage drop arising from R_{Pt} and R_d. The slope of C_μ provides information related to the distribution of traps on the TiO_2 surface.[30] The slope of C_μ is similar for the three

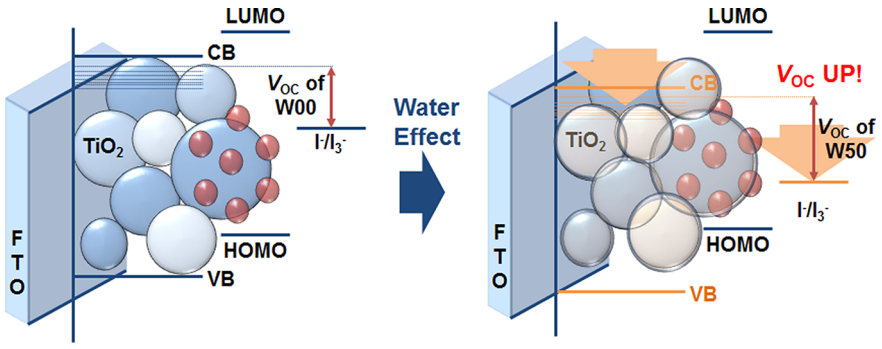

Scheme 1. Effects of water content in electrolyte on E_{redox} of I^-/I_3^- and on the conduction band of the TiO_2 electrode.

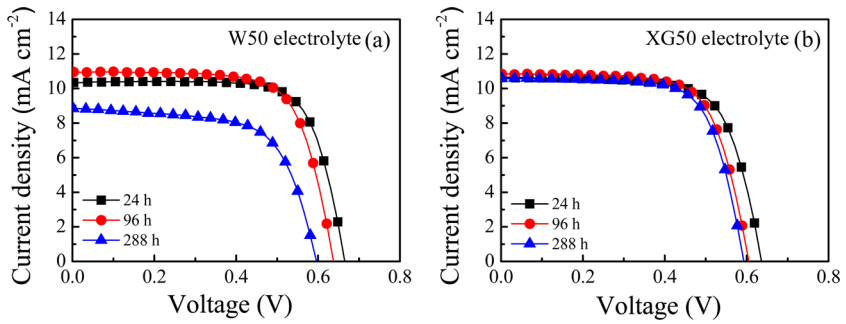

Figure 5. *J*–*V* curves for DSSCs employing (a) W50 and (b) XG50 after being stored at 65 °C and 85% relative humidity and at dark conditions for 24, 96, and 288 h.

kinds of electrolyte, as shown in Figure 4a, indicating that the water content of the electrolyte did not significantly change the distribution of traps on the surface of the TiO_2 electrode. However, at the same C_μ, V_F was negatively shifted by 118 and 75 mV for the W50 and XG50 electrolytes, respectively. This trend is consistent with that for V_{oc} for each electrolyte, as listed in Table 1. Since E_{redox} was positively shifted by 200 mV, as calculated from the CV data, the conduction band of the TiO_2 electrode was positively shifted by 82 and 125 mV for the W50 and XG50 electrolytes, respectively. Because MPN is an aprotic solvent, the conduction band of the TiO_2 electrode may positively shift by adding a protic solvent, *i.e.*, water, to the electrolyte.[3−5,20] The effects of water in the electrolyte on E_{redox} and the conduction band of the TiO_2 electrode are illustrated in Scheme 1. Both E_{redox} of the electrolyte and the conduction band potential of the TiO_2 electrode positively shift for electrolytes containing water; however, the magnitude of the shift was greater for E_{redox} than for the conduction band potential, resulting in enhanced V_{oc}. Figure 4b shows R_{ct} for each electrolyte on the basis of V_F. R_{ct} was greatly enhanced by adding water to the electrolyte, which was attributed to water molecules surrounding the TiO_2 surface and blocking I_3^- molecules from approaching the TiO_2 surface.[4,5,20] The increased R_{ct} can contribute to the enhanced V_{oc} and FF. As for the different degree of TiO_2 conduction band shift between the XG50 system and the W50 system, it is conjectured that the interactions between xanthan gum molecules and ions in the XG50 electrolyte make the surface charge of the TiO_2 electrode more positive or less negative than those in the W50 electrolyte. To clarify the exact reason for that, a further detailed investigation may be required.

Long-Term Stability. Figure 5 compares the *J*–*V* curves of the DSSCs employing each electrolyte (W50, XG50) after being stored for 24, 96, and 288 h. Each cell was stored under dark conditions at 65 °C and 85% relative humidity. Under such conditions, the water in the electrolyte can accelerate desorption of dye molecules from the TiO_2 electrode. In addition, the water in the electrolyte can decrease the adhesion between the electrode and the sealant, resulting in the sealant becoming loose and the solvent leaking from the DSSC.[9−12] As a result, the Eff of the DSSC employing W50 decreased by about 48% (from 5.06% to 3.43%) after 288 h. The Eff of the DSSC employing XG50, on the other hand, decreased by only about 7% (from 4.75% to 4.40%) after 288 h, indicating that XG50 has an enhanced long-term stability. The possible reasons for this result are that the xanthan gum in the electrolyte may have prevented the solvent from leaking from the DSSC and that the xanthan gum may have decreased the number of dye molecules desorbed from the TiO_2 electrode at high temperature. A further detailed study on the long-term stability is under way.

CONCLUSIONS

In summary, we developed a water-based polymer gel electrolyte containing xanthan gum. Owing to the

thixotropic property of the xanthan gum, it was possible to infiltrate the polymer gel electrolyte into the mesoporous TiO_2 electrode with sufficient penetration. The effects of water in the electrolyte on the photovoltaic properties of DSSCs were examined in detail from CV curves and impedance spectra. By addition of water into the electrolyte, the V_{oc} was enhanced despite the positive shift in the conduction band potential for the TiO_2 electrode; the enhanced V_{oc} was mainly due to the greater positive shift in the I^-/I_3^- redox potential. However, the water in the electrolyte decreased J_{sc} because the water desorbed dye molecules from the TiO_2 electrode and decreased the diffusion coefficient of the electrolyte. The water-based gel electrolyte exhibited comparable photovoltaic performances and significantly enhanced stability compared to the water-based liquid electrolyte. These results indicate that the water-based polymer gel electrolyte containing xanthan gum is a suitable material for practical use, which satisfies both the environmentally friendliness and the long-term stability. In addition, the effects of water in the electrolyte on DSSCs, as investigated in this study, will provide great insight for future research on water-based electrolytes.

METHODS

Preparation of Electrolytes. The reference liquid electrolyte (W00) was prepared by mixing 1.96 M propyl-methyl-imidazolium iodide (PMII), 0.15 M iodide (I_2), 0.75 M 4-*tert*-butylpyridine (TBP), and 0.1 M guanidinium thiocyanate (GSCN) in 3-methoxypropionitrile (MPN). The composition of the water-based liquid electrolyte (W50) was the same as that of W00 except that its solvent was a mixture of MPN and water (weight ratio of MPN to water = 1:1). The polymer gel electrolyte (XG50) was prepared by mixing a 3-wt % xanthan gum ($M_w = 2 \times 10^6$, product no. 0-1-A, Nisshin Oillio, Japan) aqueous solution with a solution of 4 M PMII, 0.3 M I_2, 1.5 M TBP, and 0.2 M GSCN in MPN (weight ratio of xanthan gum solution to MPN solutions = 1:1).

Fabrication of DSSCs. The fluorine-doped tin oxide glass substrates were washed with ethanol. The TiO_2 electrodes were prepared as described in a previous paper.[31] Briefly, a transparent paste was prepared using nanocrystalline TiO_2 with a 20 nm diameter that was synthesized by a hydrothermal method. A scattering paste was prepared using TiO_2 particles with a 500 nm diameter (G2, Showa Denko, Japan). First, the transparent paste was coated on an FTO glass substrates by a doctor blade method with 3M tapes as a spacer, followed by coating of the scattering paste by the same method. The prepared electrodes were sintered at 500 °C for 30 min in air. The sintered TiO_2 electrodes were dipped into a $TiCl_4$ solution (0.04 M) at 70 °C for 30 min and were resintered at 500 °C for 30 min. The thickness of the prepared electrode for the transparent, scattering, and total layer is 12, 7, and 19 μm, respectively, which were measured by an Alpha-Step IQ surface profiler (KLA Tencor). After they were cooled to 80 °C, they were dipped into a 0.3 mM solution of *cis*-bis(thiocyanato)(2,2′-bipyridyl-4,4′-dicarboxylato){4,4′-bis[2-(4-hexylsulfanylphenyl)vinyl]-2,2′-bipyridine} ruthenium(II)-mono-(tetrabutylammonium) salt (TG6 dye, One-material Organic) in a mixture of 2-methyl-2-propanol and acetonitrile (volume ratio = 1:1) at 4 °C overnight. A counter electrode was prepared by spreading a 7 mM solution of H_2PtCl_6 dissolved in 2-propanol onto an FTO glass substrate, which was subsequently dried and annealed at 450 °C for 30 min. Two small holes were drilled into the counter electrode to introduce the electrolyte, and 60 μm thick Surlyn (DuPont 1702) was used to assemble the finished counter electrode with the working electrode.

Characterization. The viscosity of the xanthan gum solution was measured using a cone/plate-type viscometer (DV-II+ Pro, Brookfield) at room temperature. The cyclic voltammograms for the electrolytes were recorded on an electrochemical analyzer (CH Instruments Inc., Austin, TX, USA) with two Pt plates as counter and working electrodes and an Ag/AgCl reference electrode. The electrolyte used for the cyclic voltammetry measurements was an MPN solution containing 0.1 M $LiClO_4$, 5 mM LiI, and 0.5 mM I_2 with and without water content (water concentration was 50 wt %). The CV curves were measured at a scan rate of 50 mV s^{-1}. The current density *versus* voltage ($J-V$) characteristics of the DSSCs were measured using a Keithley model 2400 source measure unit. A solar simulator with a 1000 W xenon lamp (Yamashida Denso) equipped with a KG-3 filter served as a light source, where the light intensity was adjusted with a National Renewable Energy Laboratory (NREL)-calibrated Si solar cell to approximate AM 1.5G and the 1 sun condition. The active area for each cell was 0.40−0.45 cm^2. A mask that had a proper active size was placed as a cover over a cell to exclude diffused light during measurements. The active cell area was measured using an image analysis program equipped with a digital microscope camera (Moticam 1000). An incident photon-to-current conversion efficiency (IPCE) system (PV Measurements, Inc.) specially designed for DSSCs was used to measure the IPCE as a function of wavelength from 300 to 800 nm. The electrochemical impedance spectra (EIS) were measured using a potentiostat (Solartron 1287) in the dark by sweeping the applied potential. The frequency ranged from 10^{-1} to 10^6 Hz. The impedance parameters were determined using Z-view software to fit the impedance spectra. Symmetric dummy cells produced with two identical Pt-coated FTO glass substrates were assembled using 60 μm thick Surlyn (DuPont 1702) to measure the diffusion coefficients of the electrolytes. For the long-term stability test, the DSSCs were stored in a humidity chamber in the dark state for 300 h. The temperature and relative humidity in the chamber were 65 °C and 85%, respectively.

Conflict of Interest: The authors declare no competing financial interest.

Acknowledgment. This research was supported by the Global Frontier R&D Program on Center for Multiscale Energy System (2012M3A6A7054856), the Pioneer Research Program (2012-0005955), the Strategic Research Program (2010-0029106), and 2013 University-Institute cooperation program funded by the National Research Foundation under the Ministry of Science, ICT & Future Planning, Korea. This work is also supported by a KIST internal project (2E23821).

Supporting Information Available: Thixotropic behavior of water-based polymer gel electrolyte containing xanthan gum, photovoltaic parameters of DSSCs according to water concentration, normalized amount of dye adsorbed per unit area and J_{sc} according to water concentration, and chemical capacitance and charge recombination resistance for TiO_2 electrode employing different kinds of electrolyte according to bias voltage. This material is available free of charge *via* the Internet at http://pubs.acs.org.

REFERENCES AND NOTES

1. O'Regan, B.; Grätzel, M. A Low-Cost, High-Efficiency Solar Cell Based on Dye-Sensitized Colloidal TiO_2 Films. *Nature* **1991**, *353*, 737–740.
2. Yella, A.; Lee, H. W.; Tsao, H. N.; Yi, C.; Chandiran, A. K.; Nazeeruddin, M. K.; Diau, E. W.; Yeh, C. Y.; Zakeeruddin, S. M.; Grätzel, M. Porphyrin-Sensitized Solar Cells with Cobalt (II/III)-Based Redox Electrolyte Exceed 12% Efficiency. *Science* **2011**, *334*, 629–634.
3. Law, C.; Pathirana, S. C.; Li, X.; Anderson, A. Y.; Barnes, P. R.; Listorti, A.; Ghaddar, T. H.; O'Regan, B. C. Water-Based

Electrolytes for Dye-Sensitized Solar Cells. *Adv. Mater.* **2010**, *22*, 4505–4509.
4. Zhu, K.; Jang, S.-R.; Frank, A. J. Effects of Water Intrusion on the Charge-Carrier Dynamics, Performance, and Stability of Dye-Sensitized Solar Cells. *Energy Environ. Sci.* **2012**, *5*, 9492–9495.
5. Jung, Y.-S.; Yoo, B.; Lim, M. K.; Lee, S. Y.; Kim, K.-J. Effect of Triton X-100 in Water-Added Electrolytes on the Performance of Dye-Sensitized Solar Cells. *Electrochim. Acta* **2009**, *54*, 6286–6291.
6. Freitas, J. N. d.; Nogueira, A. F.; Paoli, M.-A. D. New Insights into Dye-Sensitized Solar Cells with Polymer Electrolytes. *J. Mater. Chem.* **2009**, *19*, 5279–5294.
7. Chen, C. L.; Teng, H.; Lee, Y. L. *In Situ* Gelation of Electrolytes for Highly Efficient Gel-State Dye-Sensitized Solar Cells. *Adv. Mater.* **2011**, *23*, 4199–4204.
8. Kim, J. Y.; Kim, T. H.; Kim, D. Y.; Park, N.-G.; Ahn, K.-D. Novel Thixotropic Gel Electrolytes Based on Dicationic Bis-Imidazolium Salts for Quasi-Solid-State Dye-Sensitized Solar Cells. *J. Power Sources* **2008**, *175*, 692–697.
9. Harikisun, R.; Desilvestro, H. Long-Term Stability of Dye Solar Cells. *Solar Energy* **2011**, *85*, 1179–1188.
10. Pettersson, H.; Gruszecki, T. Long-Term Stability of Low-Power Dye-Sensitized Solar Cells Prepared by Industrial Methods. *Sol. Energy Mater. Sol. Cells* **2001**, *70*, 203–212.
11. Macht, B.; Turrion, M.; Barkschat, A.; Salvador, P.; Ellmer, K.; Tributsch, H. Patterns of Efficiency and Degradation in Dye Sensitization Solar Cells Measured with Imaging Techniques. *Sol. Energy Mater. Sol. Cells* **2002**, *73*, 163–173.
12. Asghar, M. I.; Miettunen, K.; Halme, J.; Vahermaa, P.; Toivola, M.; Aitola, K.; Lund, P. Review of Stability for Advanced Dye Solar Cells. *Energy Environ. Sci.* **2010**, *3*, 418–426.
13. Jin, L.; Wu, Z.; Wei, T.; Zhai, J.; Zhang, X. Dye-Sensitized Solar Cell Based on Blood Mimetic Thixotropy Sol-Gel Electrolyte. *Chem. Commun.* **2011**, *47*, 997–999.
14. Wang, Y. Recent Research Progress on Polymer Electrolytes for Dye-Sensitized Solar Cells. *Sol. Energy Mater. Sol. Cells* **2009**, *93*, 1167–1175.
15. Fang, Y.; Zhang, J.; Zhou, X.; Lin, Y.; Fang, S. A Novel Thixotropic and Ionic Liquid-Based Gel Electrolyte for Efficient Dye-Sensitized Solar Cells. *Electrochim. Acta* **2012**, *68*, 235–239.
16. O'Regan, B. C.; Walley, K.; Juozapavicius, M.; Anderson, A.; Matar, F.; Ghaddar, T.; Zakeeruddin, S. M.; Klein, C.; Durrant, J. R. Structure/Function Relationships in Dyes for Solar Energy Conversion: A Two-Atom Change in Dye Structure and the Mechanism for Its Effect on Cell Voltage. *J. Am. Chem. Soc.* **2009**, *131*, 3541–3548.
17. Matar, F.; Ghaddar, T. H.; Walley, K.; DosSantos, T.; Durrant, J. R.; O'Regan, B. A New Ruthenium Polypyridyl Dye, TG6, Whose Performance in Dye-Sensitized Solar Cells Is Surprisingly Close to That of N719, the `Dye to Beat' for 17 Years. *J. Mater. Chem.* **2008**, *18*, 4246–4253.
18. Jones, S. A.; Goodall, D. M.; Cutler, A. N.; Norton, I. T. Application of Conductivity Studies and Polyelectrolyte Theory to the Conformation and Order-Disorder Transition of Xanthan Polysaccharide. *Eur. Biophys. J.* **1987**, *15*, 185–191.
19. Lu, H.-L.; Lee, Y.-H.; Huang, S.-T.; Su, C.; Yang, T. C. K. Influences of Water in Bis-Benzimidazole-Derivative Electrolyte Additives to the Degradation of the Dye-Sensitized Solar Cells. *Sol. Energy Mater. Sol. Cells* **2011**, *95*, 158–162.
20. Liu, Y.; Hagfeldt, A.; Xiao, X.-R.; Lindquist, S.-E. Investigation of Influence of Redox Species on the Interfacial Energetics of a Dye-Sensitized Nanoporous TiO_2 Solar Cell. *Sol. Energy Mater. Sol. Cells* **1998**, *55*, 267–281.
21. Boschloo, G.; Gibson, E. A.; Hagfeldt, A. Photomodulated Voltammetry of Iodide/Triiodide Redox Electrolytes and Its Relevance to Dye-Sensitized Solar Cells. *J. Phys. Chem. Lett.* **2011**, *2*, 3016–3020.
22. Mikoshiba, S.; Murai, S.; Sumino, H.; Kado, T.; Kosugi, D.; Hayase, S. Ionic Liquid Type Dye-Sensitized Solar Cells: Increases in Photovoltaic Performances by Adding a Small Amount of Water. *Curr. Appl. Phys.* **2005**, *5*, 152–158.
23. Hagfeldt, A.; Sun, G. B.; Kloo, L.; Pettersson, H. Dye-Sensitized Solar Cells. *Chem. Rev.* **2010**, *110*, 6595–6663.
24. Yum, J. H.; Baranoff, E.; Kessler, F.; Moehl, T.; Ahmad, S.; Bessho, T.; Marchioro, A.; Ghadiri, E.; Moser, J. E.; Yi, C.; *et al.* A Cobalt Complex Redox Shuttle for Dye-Sensitized Solar Cells with High Open-Circuit Potentials. *Nat. Commun.* **2012**, *3*, 631–638.
25. Kim, J.-Y.; Kim, J. Y.; Lee, D.-K.; Kim, B.; Kim, H.; Ko, M. J. Importance of 4-*tert*-Butylpyridine in Electrolyte for Dye-Sensitized Solar Cells Employing SnO_2 Electrode. *J. Phys. Chem. C* **2012**, *116*, 22759–22766.
26. Raga, S. R.; Barea, E. M.; Fabregat-Santiago, F. Analysis of the Origin of Open Circuit Voltage in Dye Solar Cells. *J. Phys. Chem. Lett.* **2012**, *3*, 1629–1634.
27. Fabregat-Santiago, F.; Garcia-Belmonte, G.; Mora-Sero, I.; Bisquert, J. Characterization of Nanostructured Hybrid and Organic Solar Cells by Impedance Spectroscopy. *Phys. Chem. Chem. Phys.* **2011**, *13*, 9083–9118.
28. Stergiopoulos, T.; Kontos, A. G.; Likodimos, V.; Perganti, D.; Falaras, P. Solvent Effects at the Photoelectrode/Electrolyte Interface of a DSC: A Combined Spectroscopic and Photoelectrochemical Study. *J. Phys. Chem. C* **2011**, *115*, 10236–10244.
29. Góes, M. S.; Joanni, E.; Muniz, E. C.; Savu, R.; Habeck, T. R.; Bueno, P. R.; Fabregat-Santiago, F. Impedance Spectroscopy Analysis of the Effect of TiO_2 Blocking Layers on the Efficiency of Dye Sensitized Solar Cells. *J. Phys. Chem. C* **2012**, *116*, 12415–12421.
30. Wang, Q.; Ito, S.; Grätzel, M.; Fabregat-Santiago, F.; Mora-Sero, I.; Bisquert, J.; Bessho, T.; Imai, H. Characteristics of High Efficiency Dye-Sensitized Solar Cells. *J. Phys. Chem. B* **2006**, *110*, 25210–25221.
31. Koo, H.-J.; Park, J.; Yoo, B.; Yoo, K.; Kim, K.; Park, N.-G. Size-Dependent Scattering Efficiency in Dye-Sensitized Solar Cell. *Inorg. Chim. Acta* **2008**, *361*, 677–683.